

## MODELLING THE EFFECT OF SLOSHING ON SHIP MOTIONS

### DRAFT

**Tim Bunnik**  
MARIN

Wageningen, The Netherlands

**Arthur Veldman**

University of Groningen  
Groningen, The Netherlands

#### ABSTRACT

Ships with partially filled liquid tanks, such as LNG carriers or FPSOs, are sensitive to sloshing in case they are exposed to waves. The effect of sloshing can have a pronounced effect on the ship motions, in particular roll in oblique seas. In this paper several methods are described which can be used to quantify this effect. The first is a linear diffraction method in which the effect of the liquid in the tank is modeled as a solid inertia of the fluid mass, an added mass and damping of the sloshing fluid and a hydrostatic free-surface correction to the GM. The response is easily computed in the frequency domain. The second is a time domain method in which the sloshing liquid in the tank is modeled with the CFD code ComFLOW. The forces exerted by the liquid on the tank walls is included in a time-domain simulation of the ship motions, based on linear potential flow for the outer domain (ship hull and ocean). The computed ship motions are again input for the motions of the liquid tank, generating a 2-way coupling between the dynamics of the tank and the ship. Both methods are applied to sloshing model tests, published by Molin (2008). In these tests, the response of a barge was measured with a completely filled and partially filled tank in beam seas. The results of the linear diffraction method agree reasonably well, but some differences in the roll response near the first sloshing mode are observed. The coupled time-domain method gives very good results for both low and high sea states.

#### INTRODUCTION

In the coming years, the trading of liquefied natural gas (LNG) is expected to increase significantly worldwide. This has led to an increased interest in the potential for developing

FPSO LNG facilities. At these facilities, LNG is transferred in a complex offloading operation from the FPSO to LNG carriers. This is repeated in near-shore facilities where the LNG is re-gasified and transferred to shore. A very important factor in the downtime of these offloading operations is the wave induced motion of the FPSO and the LNGC. During these operations, which may take up to 24 hours, filling rates of the containment system may slowly vary between empty to completely filled, or the other way around. In case of partially filled containment systems, LNG sloshing may occur which can heavily affect the wave-induced motions of the vessels, especially roll. This may therefore occur during a significant part of the offloading operation and have a large effect on the downtime of the operation. The large effect of liquid sloshing in partially filled tanks on roll motions has been shown experimentally by amongst others Molin (2008), Gaillarde (2004) and Francescutto and Contento (1994).

Several authors have published methods to account for the effect of sloshing on ship motions. Based on linear potential theory, frequency domain formulations were developed by various authors to study the interaction effect between ship motions and sloshing (Malenica et. al. (2003), Molin et. al. (2002), Huang et. al. (2009), Booki Kim and Yung S. Shin (2008)). Time-domain coupling using CFD for the sloshing tank were developed and published by Seokkyu Cho et. al. (2008), Booki Kim and Yung S. Shin (2008) and Yongwhan Kim (2002).

In this paper, two different models are presented that take into account the effect of sloshing on ship motions:

1. A linear diffraction method in which both the liquid motions in the containment system and the liquid motions outside the vessel are described by linear potential flow in the frequency domain.
2. A time-domain coupling method in which the sloshing liquid in the containment system is computed by CFD

(Volume of Fluid method) and the ship hydrodynamics by means of linear diffraction theory.

Both methods are applied to model tests described by Molin (2008), in which he measured the motion response of a barge with a partially filled water container on deck.

## LINEAR DIFFRACTON METHOD

Linear diffraction theory is at present still the basis for nearly all the design tools in the offshore industry. It certainly has considerable limitations like:

- Viscous effects are neglected
- There is no rotation in the fluid
- It is only valid for small ship motions and waves (linearization of boundary conditions)

Still, it has shown to give good results even beyond the limits for which it has in theory been designed. Therefore, it was investigated if this method can be useful in predicting the effect of sloshing loads on ship motions.

In order to make the selected linear diffraction code (MARIN's DIFFRAC program) suitable for the evaluation of liquid motions in closed tank, the following modifications were made:

- The hydrostatics restoring forces of the sloshing tank are computed and added to the hydrostatic restoring forces of the ship. These are given by (Malenica et. al. (2003)):

$$C = -\rho g \begin{pmatrix} 0 & 0 & 0 & 0 & 0 & 0 \\ 0 & 0 & 0 & 0 & 0 & 0 \\ 0 & 0 & 0 & 0 & 0 & 0 \\ 0 & 0 & 0 & I_{11}^{AA} & I_{12}^{AA} & 0 \\ 0 & 0 & 0 & I_{21}^{AA} & I_{22}^{AA} & 0 \\ 0 & 0 & 0 & 0 & 0 & 0 \end{pmatrix}$$

Where  $I_{11}^{AA}$ ,  $I_{12}^{AA}$ ,  $I_{22}^{AA}$ ,  $I_{21}^{AA}$  are the area moments of the waterplane with respect to the centre of the free surface. It can be seen that the tank has a de-stabilising effect (negative spring term), often referred to as the GM free-surface correction.

- An additional forcing term in the free-surface condition for the sloshing tank is included (Malenica et. al. (2003)), which arises from the fact that the free surface is moving due to the motions of the ship:

$$\frac{\partial \varphi}{\partial z} - \frac{\omega^2}{g} \varphi = -i\omega f_j$$

$$f_j = \begin{cases} 0 & j = 1 & (\text{surge}) \\ 0 & j = 2 & (\text{sway}) \\ 1 & j = 3 & (\text{heave}) \\ Y_{AT} & j = 4 & (\text{roll}) \\ -X_{AT} & j = 5 & (\text{pitch}) \\ 0 & j = 6 & (\text{yaw}) \end{cases}$$

$(X_{AT}, Y_{AT})$  is the centre of the free surface.

Since nonlinearities and viscous effects are neglected diffraction results highly overestimate the liquid motions at the natural sloshing frequencies of the sloshing tank. The added mass tends to infinity there. Another feature is that the damping is zero since all the wave energy remains inside the closed tank. A trick to smoothen the peak in the added mass and to add damping is to include a dissipation term in the free-surface condition of the tank. The following condition is applied:

$$\frac{\partial \varphi}{\partial z} - (1 + i\epsilon) \frac{\omega^2}{g} \varphi = -i\omega f_j \quad (\text{equation 1})$$

Where  $\epsilon$  is a non-dimensional damping value. This condition is the same as used by several authors (Bunnik et. al. (2009), Chen (2005)) to suppress resonant free-surface motions in the gap between side-by-side offloading vessels.

Summarizing, the sloshing fluid in the tank is modeled as:

1. A solid homogeneous mass with solid inertia loads
2. A frequency dependent added mass and possibly damping
3. A (negative) hydrostatic restoring force.

These loads are added to the equation of motion of the ship, which results in the motion response in the frequency domain.

## TIME-DOMAIN METHOD

To account for non-linear effects, CFD can be applied. However, CFD is not yet robust, practical and fast enough to model simultaneously an entire moving ship in an external fluid and the sloshing tank. Therefore, an approach was adopted where the sloshing tank was modeled with CFD, and the ship hydrodynamics with linear potential flow. In this manner, non-linear sloshing effects are taken into account, but non-linear ship hydrodynamics are not. This is thought to be a good approach since the main focus here is on offloading operations. The related operational sea states result in more or less small ship motions (justifying the linear approach), whereas non-linear sloshing effects may already occur in these sea states, especially if the ship is moving at frequencies near the natural sloshing modes of the sloshing tank. The use of such an approach in high sea states (for example a sailing LNG carrier with partially filled tanks in rough weather) is questionable.

The CFD method that was used is the Volume of Fluid (VoF) method ComFLOW, developed by the University of Groningen. This method has extensively been used and validated in the past for sloshing loads on containment systems using pre-defined motions (Wemmenhove (2008)). The method has been extended such that it can now be coupled to other time-domain codes and the motions of the sloshing tank can interactively be controlled. This situation is sketched in Figure 1.

The coupling has been established using the MARIN time-domain ship motion code aNySIM. aNySIM applies impulse-

response theory to compute ship motions in the time-domain, based on the following equation of motion:

$$\sum_{j=1}^6 (M_{kj} + m_{kj}) \ddot{x}_j + \int_{-\infty}^t R_{kj}(t-\tau) \dot{x}_j(t-\tau) d\tau + C_{kj} x_j = F_k(t)$$

Where

$x_j$	=	motion mode $j$
$F_k(t)$	=	external force mode $k$
$M$	=	solid inertia matrix
$m$	=	added inertia matrix
$C$	=	matrix of hydrostatic restoring forces
$R$	=	matrix of retardation functions

The external force includes the loads due to sloshing. The coupling is explicit, which means that both methods are running with information from the other method's previous time step. The methods are forced to exchange information at communication time levels with constant time step in between. In detail, the explicit coupling works as follows:

- aNySIM computes the accelerations, velocities and motions of the ship by integrating the equation of motion from the present communication time level to the next. During this time step it keeps the sloshing loads it has received from the CFD code constant until it has reached the next communication time level.
- The CFD method is then progressed towards the next communication time level. The motions, velocities and accelerations are extrapolated linearly one time step into the future and are prescribed to the tank during its march in time. The internal time step of the CFD code is in general much smaller than the communication time step.
- When the CFD code has reached the next communication time level, the sloshing loads are computed. These are again used in the equation of motion of the ship to progress aNySIM towards the present communication time level.

## RESULTS: COMPARISON WITH EXPERIMENTS

Experimental results from Molin (2008) were used to validate both methods. In these experiments, a barge with a container of water on deck was exposed to beam seas. The container of water has a moveable ceiling and tests were done with the ceiling on top of the water (no free surface motions) and the ceiling lifted above the free surface, making free-surface motions (sloshing) possible. Figure 2 shows a photo of the model tests. The test results, barge and tank geometry and weight distribution are well described in the paper, making the results perfectly suited for validation of the methods presented in this paper.

Figure 3 shows the roll RAO of the barge, derived from the measured roll motions in the experiments, with and without airgap in the water container. It can be noticed that:

1. Without airgap, the roll RAO has a single peak at the natural frequency.
2. With airgap, the RAO has a double peak. The left peak is the natural frequency which has shifted towards a lower frequency due to loss of hydrostatic stability. The right peak is induced by sloshing dynamics near the first sloshing mode.

Figure 4 shows the roll RAO, derived from the measured roll motions in the experiments. It shows one of the main findings from the experiments; The 2<sup>nd</sup> (sloshing-induced) peak is heavily affected by the height of the sea state. It collapses if the significant wave height is doubled from  $H_s=0.06$ m to  $H_s=0.12$  m. Molin attributes this to non-linear free-surface effects in the water container.

Figure 5 shows the panel distribution that was used in the diffraction analysis for the barge and the sloshing tank. A separate diffraction analysis was carried out for the sloshing tank and the barge. The results for the sloshing tank (added mass and damping) was added to the results of the barge afterwards.

The diffraction analysis results in a very large added mass near the odd ( $n=1,3,5 \dots$ ) sloshing modes. The sloshing modes in a rectangular tank are given by:

$$k_n = \frac{n\pi}{B} \quad n = 1,2,3, \dots$$

$$\lambda_n = \frac{2B}{n}$$

$$\omega_n^2 = g k_n \tanh k_n h$$

Where

$k_n$	=	wave number	[1/m]
$B$	=	tank width	[m]
$\lambda_n$	=	wave length	[m]
$\omega_n$	=	wave frequency	[1/s]
$h$	=	water depth	[m]

For the first sloshing mode,  $\frac{1}{2}$  a wave length fits into the width of the tank. For the second sloshing mode, 1 wave length fits into the width of the tank. The wave profiles in the tank for the 1<sup>st</sup> and 2<sup>nd</sup> sloshing mode are given in Figures 6 and 7. The 2<sup>nd</sup> sloshing mode is not directly excited by tank motions, since the velocity distribution in this standing wave does not match any velocity profile on the tank boundary resulting from tank motions. If this mode exists it is mainly due to non-linear wave interaction in the tank. In linear theory this sloshing mode therefore does not show up in the results.

Figure 8 shows the combined added mass from the barge and the tank. It can be seen that the added mass becomes very large at the first sloshing mode, since there is no damping to suppress the resonant water motions in the tank. Therefore, the effect of adding an additional dissipation term in the free surface condition (equation 1) was investigated. Figure 8 shows

that the added mass can be brought back to more realistic values using this additional dissipation term. However, this parameter needs tuning by means of model test results or CFD computations which are not always available.

Figure 9 shows the roll RAO computed by a diffraction analysis when there is no airgap in the tank (ceiling is on the free surface). As expected, a good agreement with the model tests is obtained. It should be mentioned that the viscous damping on the barge hull was tuned to give the proper amplitude at the natural frequency.

Figure 10 shows the roll RAO computed by a diffraction analysis when there is an airgap in the tank (ceiling is above the free surface). Several values of the free-surface dissipation term were used. It can be seen that:

- The response becomes double-peaked like in the experiments.
- The location of the first (left, lowest frequency) peak is correct, but the peak is somewhat too wide.
- The location of the second (right, highest frequency) peak is not correct. It is located at  $\omega=6.3$  rad/s instead of  $\omega=6.5$  rad/s. Also, the peak is less wide.
- The additional dissipation term reduces the height of the peak, but not the location.

A diffraction analysis can give a global idea of the roll response in case of sloshing and may be sufficient for a first “engineering” analysis. However, for more detailed design a more accurate prediction is needed.

Figures 11, 12 and 13 show the three different grids that were used in the CFD analysis for the tank, which was coupled to the time-domain analysis of the barge motions. A very coarse grid was first used (20x12) and then refined to a coarse grid (40x23) and a fine grid (80x46). It should be noted that always, 1 cell was used in the longitudinal direction of the barge. This means tank sloshing in the longitudinal direction is neglected. This is a fair assumption since only beam seas are considered here.

Figure 14 shows the roll response of the barge when there is no air gap in the tank (so no free-surface motions). The lowest sea state (irregular 1) from the paper by Molin (2008) was used:

Hs	=	0.06	m
Tp	=	1.6	s
Spectrum type	=	JONSWAP	
$\gamma$	=	2	

The roll response was derived from the computed roll motion time trace for a simulation duration of 400 s, which is similar to the duration of the model tests. In all simulations, the communication time step between the CFD model and the simulation model for the barge motions was set at  $\Delta t = 0.005$  s (200 Hz). A good agreement between the CFD coupling and the model tests is obtained, although the results are slightly overestimated for frequencies between 5 and 7 rad/s. The viscous roll damping of the barge was taken the same as for the diffraction coupling.

Figure 15 shows the roll response with an air gap of 16 cm (for the sea state just mentioned). A very good agreement between the model tests and the simulations is found, also for the 2<sup>nd</sup>, sloshing-induced peak in the response. Already with a very coarse grid, good results are obtained. The effect of grid refinement is surprisingly small. The CPU time for the coarsest grid is about 1 hour, making such an approach well suited for engineering studies. Figure 17 shows a snapshot of the free surface in the tank. Roof impacts do not occur in this situation.

Figure 16 shows the roll response with an air gap of 16 cm, but now for sea state irregular 3, which has a twice as high Hs:

Hs	=	0.12	m
Tp	=	1.6	s
Spectrum type	=	JONSWAP	
$\gamma$	=	2	

A good agreement between the model tests and the simulations is found. A large reduction of the second peak is found, very similar to the model tests. The height of the peak is slightly overestimated. The height of the first peak is overestimated. This is because the same linear viscous damping value for the barge was used as for the lower sea state. In reality, the damping is probably non-linear and a higher damping should be used for higher sea states.

There is more effect of grid refinement for this higher sea state. This is quite logical since a finer grid is needed to accurately capture the steeper waves. Figure 18 shows a snapshot of the free surface in the tank. Roof impacts often occur in this situation. However, Molin (2008) shows that this has only a small effect on the roll response.

## CONCLUSIONS

Two different methods for the simulation of the effect of sloshing in cargo tanks on ship motions were presented:

1. A combined linear diffraction analysis for the tank and the ship.
2. A CFD model for the tank coupled to a linear-diffraction based time-domain analysis of the barge motions.

The two methods were validated with experiments published by Molin (2008) in which the response of a barge in beam seas was measured with a container of water on deck. The validation shows that:

- A reasonable agreement is found between the resulting roll RAOS from diffraction model and the experiments. The 2<sup>nd</sup> sloshing-induced peak in the response is slightly shifted and the peak is less wide than in the experiments. Additional dissipation on the tank free-surface has to be applied to obtain realistic added mass values and roll response.
- A very good agreement is found between the coupled CFD-diffraction model and the experiments. A grid refinement study shows that already on very coarse grids good results can be obtained.
- In higher sea states, the 2<sup>nd</sup> peak in the roll response becomes significantly lower. This effect is also

predicted by the coupled CFD-diffraction model, although the response is slightly over estimated.

Although the coupled CFD-diffraction model is giving good results for this particular application of a large free-surface tank, it certainly has its limitations:

- The ship model is based on linear diffraction. For higher sea states (for example an LNG carrier sailing in rough weather) this is insufficient and a more advanced model should be used.
- Coarse grids are used without any resolution in boundary layers. Viscous effects are therefore not resolved. When viscous effects start playing a role, refined boundary layers and turbulence models should be used. This is at present not possible with the CFD model that was used for this paper.

## REFERENCES

Huang et. al. (2009), "Coupled Tank Sloshing and LNG Carrier Motions", *Proceedings of the Nineteenth International Offshore and Polar Engineering Conference*, Osaka, Japan.

Chen, XB (2005), "Hydrodynamic analysis for offshore LNG terminals", *2nd offshore hydrodynamics symposium*, Rio de Janeiro, Brazil.

Bunnik et. al. (2009), "Hydrodynamic Analysis for Side-by-Side Offloading", *Proceedings of the Nineteenth International Offshore and Polar Engineering Conference*, Osaka, Japan.

Alberto Francescutto and Giorgio Contento (1994), "An Experimental Study of the Coupling Between Roll Motion and Sloshing in a Compartment", *Proceedings of the Fourth International Offshore and Polar Engineering Conference*, Osaka, Japan.

Bernard Molin, Fabien Remy, Alain Ledoux and Nicolas Ruiz (2008), "Effect of roof impacts on coupling between wave response and sloshing in tanks of LNG-carriers", *Proceedings of the 27th International Conference on Offshore Mechanics and Arctic Engineering*, Lisbon, Portugal.

Malenica et. al. (2003), "Dynamic coupling of seakeeping and sloshing", *Proceedings of the Thirteenth International Offshore and Polar Engineering Conference*, Honolulu, USA.

Rik Wemmenhove (2008), "Numerical Simulation of two-phase flow in offshore environments", PhD thesis, Rijksuniversiteit Groningen.

Seokkyu Cho et. al. (2007), "Studies on the Coupled Dynamics of Ship Motion and Sloshing including Multi-Body Interactions", *Proceedings of the Seveeneenth International Offshore and Polar Engineering Conference*, Lisbon, Portugal.

Molin, B. et. al. (2002), "LNG-FPSO's: Frequency domain coupled analysis of support and liquid cargo motion", *Proceedings of the IMAM Conference*, Rethymnon, Greece.

Booki Kim and Yung S. Shin (2008), "Coupled seakeeping with liquid sloshing in ship tanks", *Proceedings of the ASME 27th International Conference on Offshore Mechanics and Arctic Engineering*, Estoril, Portugal.

Yonghwan Kim (2002), "A Numerical Study on Sloshing Flows Coupled with Ship Motion—The Anti-Rolling Tank Problem", *Journal of Ship Research*, Vol. 46, No. 1, March 2002, pp. 52-62.

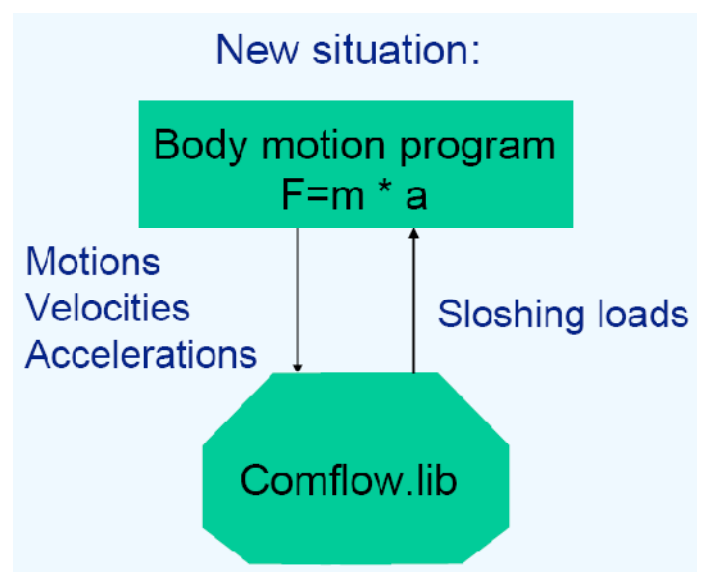


Figure 1: Time-domain coupling of CFD with body motion program.

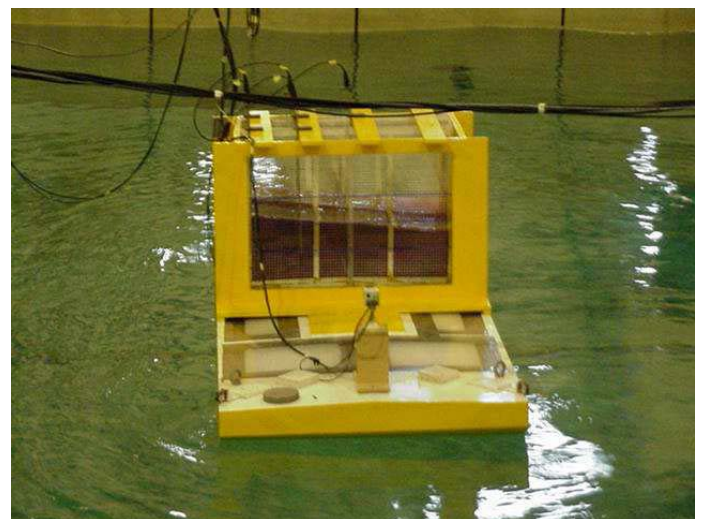


Figure 2: Photo from model tests (Molin (2008)).

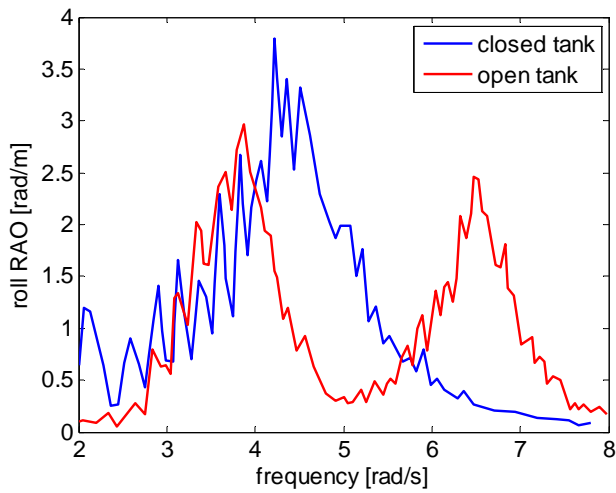


Figure 3: Barge roll response with open and closed tank (Molin (2008)).

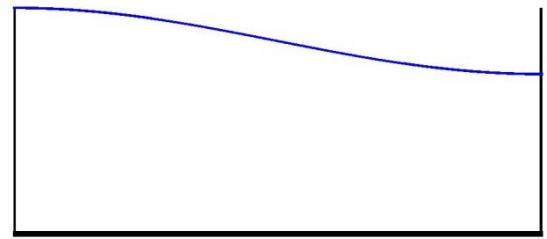


Figure 6: Wave profile for 1<sup>st</sup> sloshing mode

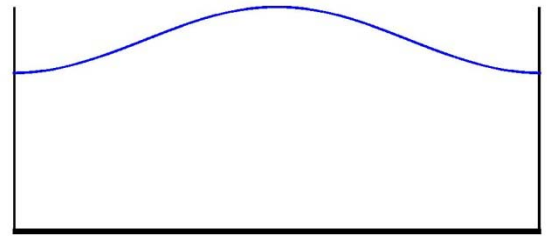


Figure 7: Wave profile for 2<sup>nd</sup> sloshing mode

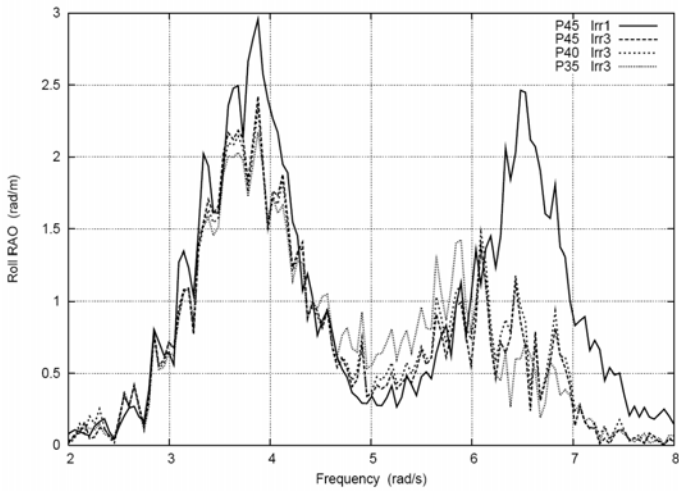


Figure 4: Barge roll response for different seastates and airgaps (Molin (2008)).

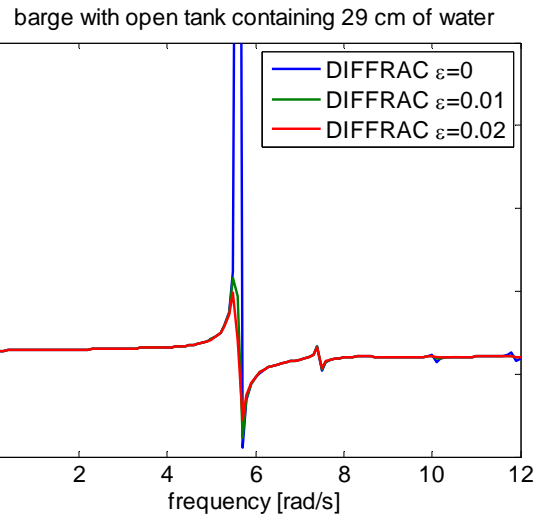


Figure 8: Roll added mass of barge+tank and effect of damping parameter.

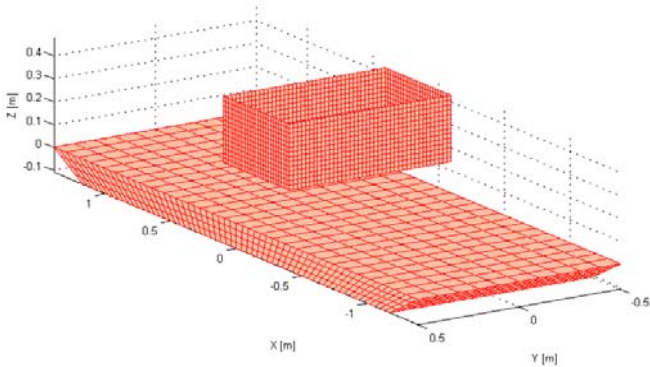


Figure 5: Panel distribution of barge and tank for linear diffraction analysis.

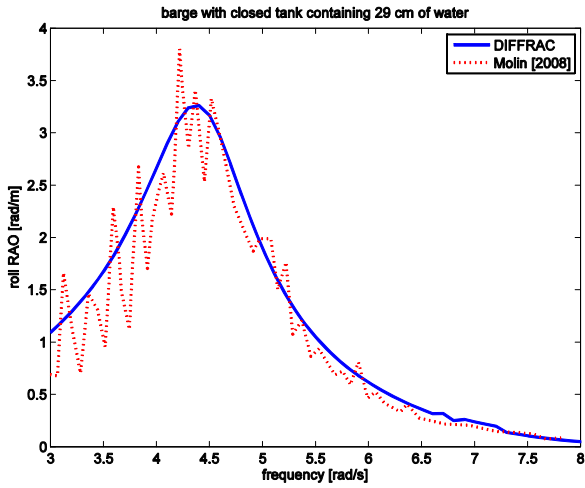


Figure 9: Roll response of barge with closed tank in seastate irr1, experimental versus linear diffraction results.

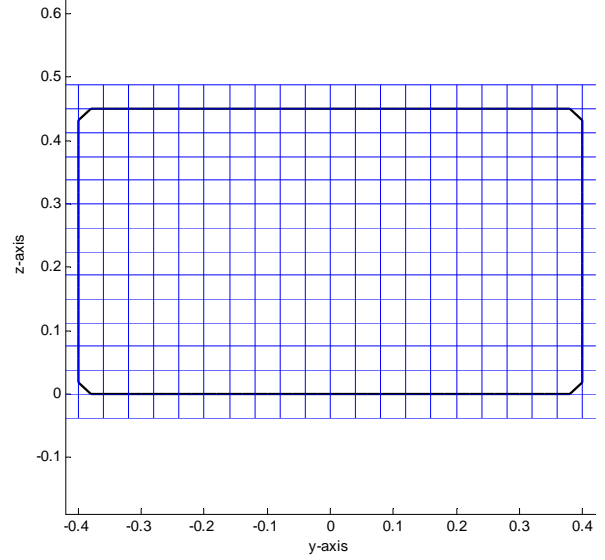


Figure 11: Very coarse 2D CFD mesh of sloshing tank (20x12).

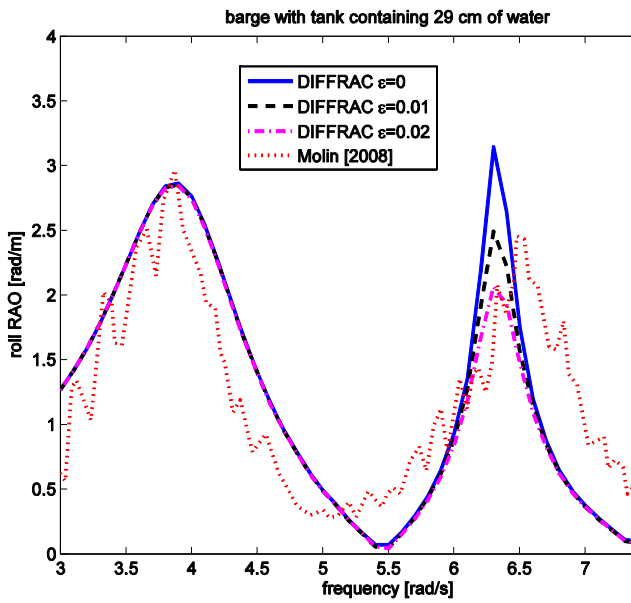


Figure 10: Roll response of barge with open tank in seastate irr1, experimental versus linear diffraction results.

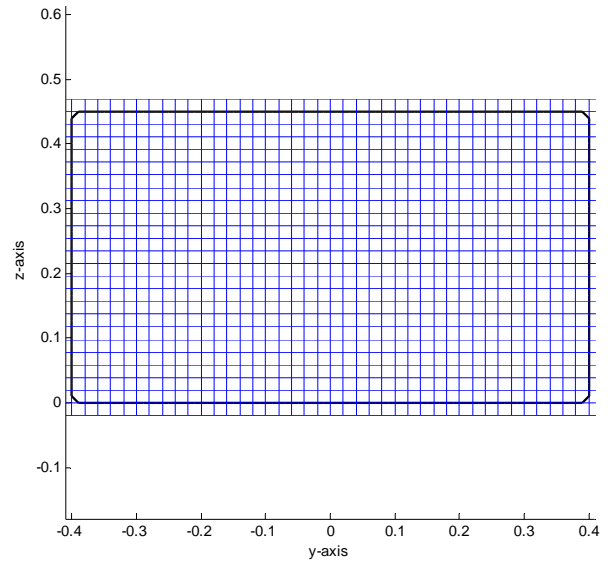


Figure 12: Coarse 2D CFD mesh of sloshing tank (40x23).

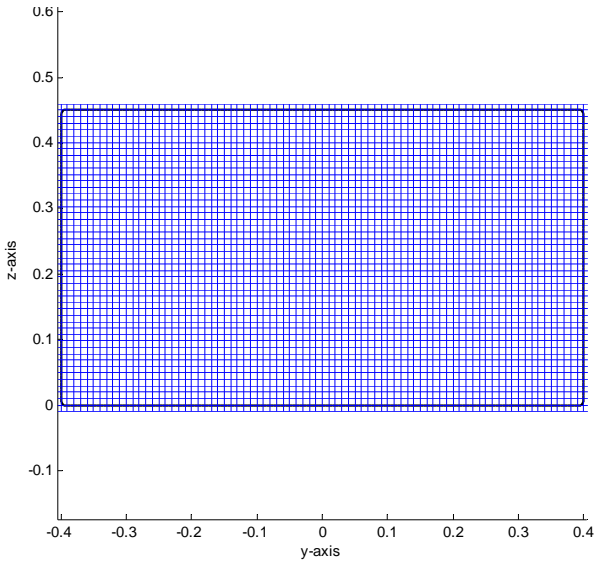


Figure 13: Fine 2D CFD mesh of sloshing tank (80x46).

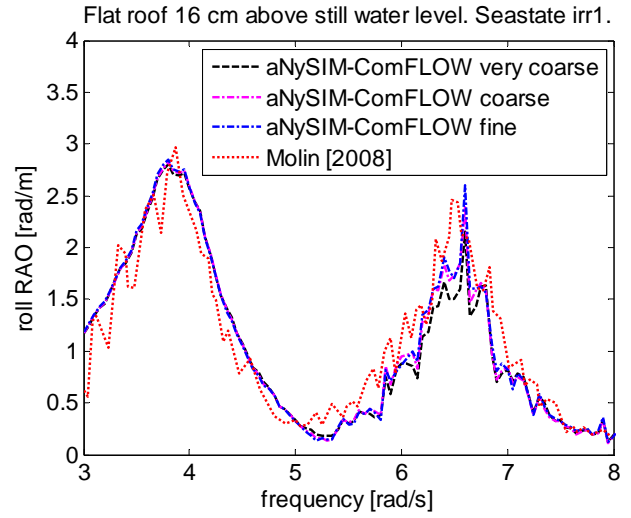


Figure 15: Roll response of barge with open tank in seastate irr1, experimental versus time-domain results.

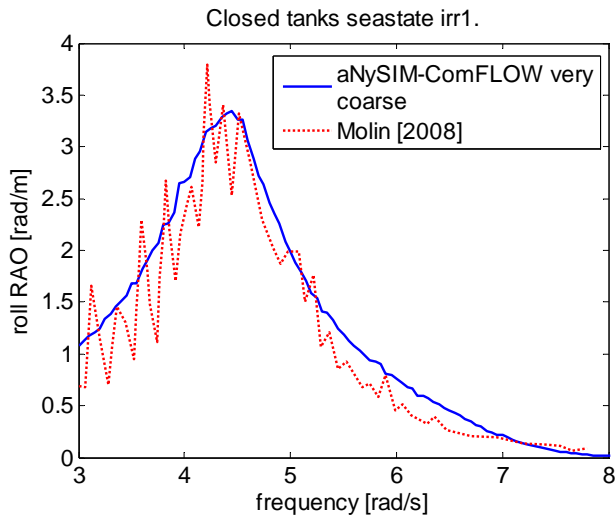


Figure 14: Roll response of barge with closed tank in seastate irr1, experimental versus time-domain results.

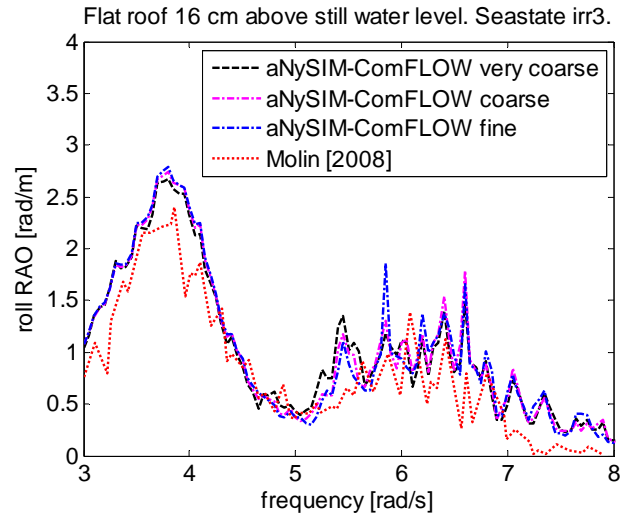


Figure 16: Roll response of barge with open tank in seastate irr3, experimental versus time-domain results.

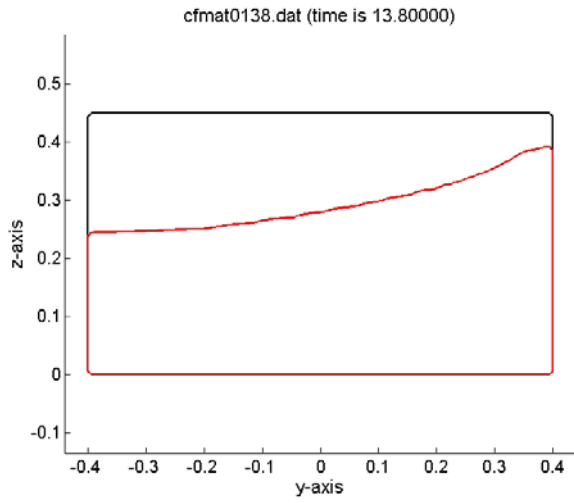


Figure 17: Snapshot of tank sloshing in sea state irregular 1.

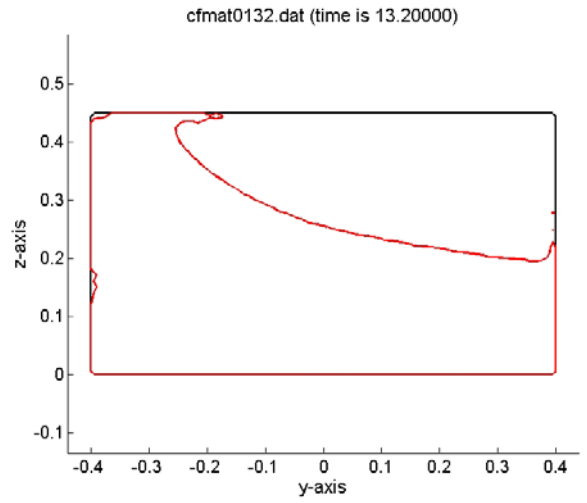


Figure 18: Snapshot of tank sloshing in sea state irregular 3.

